

## Evolution of the galaxy merger fraction in the CLAUDS+HSC-SSP deep fields

Nathalie Thibert,<sup>1</sup> Marcin Sawicki,<sup>1</sup> Andy Goulding,<sup>2</sup> Stéphane Arnouts,<sup>3</sup> Jean Coupon,<sup>4</sup> and Stephen Gwyn<sup>5</sup>

<sup>1</sup>*Institute for Computational Astrophysics and Department of Astronomy and Physics, Saint Mary's University, Halifax, NS, B3H 3C3, Canada*

<sup>2</sup>*Department of Astrophysical Sciences, Princeton University, Princeton, NJ 08544-1001, USA*

<sup>3</sup>*CNRS, LAM - Laboratoire d'Astrophysique de Marseille, Aix Marseille Université, 38 rue F. Joliot-Curie, F-13388 Marseille, France*

<sup>4</sup>*Astronomy Department, University of Geneva, Chemin d'Ecogia 16, CH-1290 Versoix, Switzerland*

<sup>5</sup>*NRC Herzberg Astronomy and Astrophysics, 5071 West Saanich Road, Victoria, BC, V9E 2E7, Canada*

### ABSTRACT

We estimate the evolution of the galaxy-galaxy merger fraction for  $M_* > 10^{10.5} M_\odot$  galaxies over  $0.25 < z < 1$  in the  $\sim 18.6$  deg<sup>2</sup> deep CLAUDS+HSC-SSP surveys. We do this by training a Random Forest Classifier to identify merger candidates from a host of parametric morphological features, and then visually follow-up likely merger candidates to reach a high-purity, high-completeness merger sample. Correcting for redshift-dependent detection bias, we find that the merger fraction at  $z = 0$  is  $1.0 \pm 0.2\%$ , that the merger fraction evolves as  $(1+z)^{2.3 \pm 0.4}$ , and that a typical massive galaxy has undergone  $\sim 0.3$  major mergers since  $z = 1$ . This pilot study illustrates the power of very deep ground-based imaging surveys combined with machine learning to detect and study mergers through the presence of faint, low surface brightness merger features out to at least  $z \sim 1$ .

*Keywords:* galaxies: evolution — galaxies: interactions

### INTRODUCTION

Galaxy-galaxy mergers play an important role in the hierarchical structure formation paradigm as they provide avenues for galaxies to grow their stellar masses and transform their morphologies (e.g., Bundy et al. 2009; Xu et al. 2012; Conselice 2014). Though rare today, merging of similar-mass galaxies was common in the past (e.g., Le Fevre et al. 2000; Patton et al. 2002; Bridge et al. 2010; Conselice 2014; Sawicki et al. 2020). To further characterize the role of mergers over cosmic time requires samples sufficiently large to study the dependence of merging on redshift, environment, and intrinsic galactic properties such as mass, star formation rate, or AGN activity.

Distant merging galaxies can be identified as close pairs, likely to merge through dynamical friction (e.g., Patton et al. 2002; Bundy et al. 2009; Mundy et al. 2017), but this approach requires statistical background corrections or expensive spectroscopy. An alternative is to find galaxies with disturbed morphologies marking ongoing mergers (e.g., Le Fevre et al. 2000; Bridge et al. 2010). Identification of such morphological signatures can be done visually, but this is tedious for large samples and not easily reproducible. Consequently, automated approaches to morphological merger identification are attractive (e.g., Conselice et al. 2008; Lotz et al. 2008; Freeman et al. 2013; Ackermann et al. 2018; Goulding et al. 2018). Here we summarize the results of our pilot study (Thibert 2018<sup>1</sup>) that uses morphological features and a Random Forest Classifier (RFC) to pre-select merger candidates in the combined Hyper Suprime-Cam Strategic Survey Program (HSC-SSP; Aihara et al. 2018a) and CFHT Large Area U-band Deep Survey (CLAUDS; Sawicki et al. 2019) dataset.

### DATA

We use the photometric redshifts and stellar masses ( $M_*$ ) estimated from very deep  $u/u^*+grizy$  photometry of the overlapping 18.60 deg<sup>2</sup> of the CLAUDS and HSC-SSP Deep/UltraDeep regions. Our  $z_{phot}$  are described in Sawicki

Corresponding author: Marcin Sawicki  
marcin.sawicki@smu.ca

<sup>1</sup> Full text: <https://library2.smu.ca/handle/01/27980>

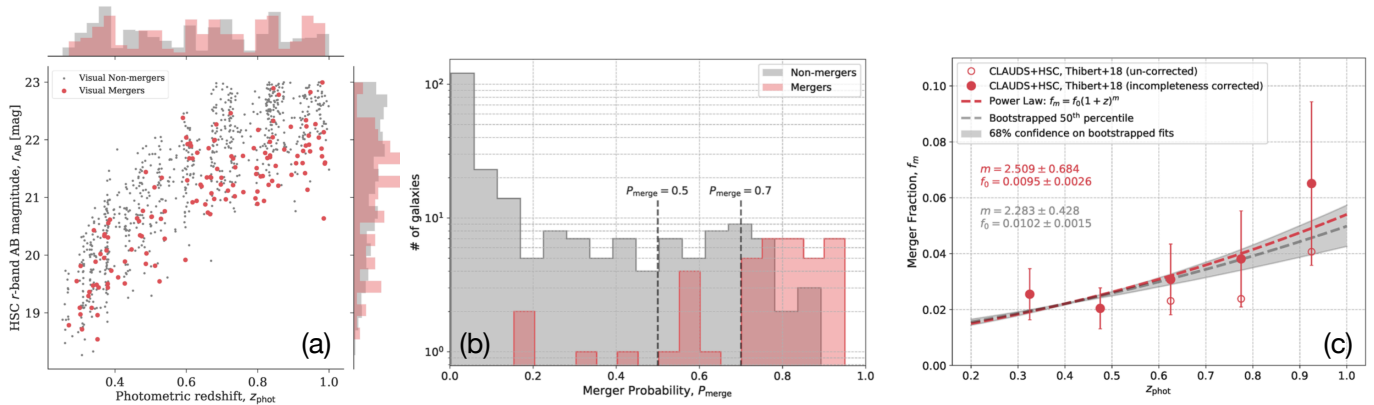


**Figure 1.** (a) Our training/testing sample; red points mark galaxies visually classified as mergers. The  $M_* > 10^{10.5} M_\odot$  cut produces the upper envelope and only at the highest redshift the  $r_{AB} < 23.0$  cut starts becoming important. (b) Distribution of merger probabilities reported by the RFC for the testing sample; red are visually-classified mergers, gray are non-mergers. (c) Merger fraction evolution. Open points denote the raw merger fraction, while closed points show the incompleteness-corrected values. The red dashed line is the power-law fit to the incompleteness-corrected points. The gray dashed line and shaded region denote the 50th percentile and 68% confidence interval from bootstrapped fits to the (incompleteness-corrected) measurements.

et al. (2019) while  $M_*$  estimates are similar to those of Moutard et al. (2020). We match this catalog to the  $r$ -band images from an internal HSC-SSP data release intermediate in depth between PDR1 and PDR2 (Aihara et al. 2018b, 2019). Visual inspection suggests that  $r_{AB} < 23.0$  is sufficient for morphological feature detection. Together with a  $M_* < 10^{10.5} M_\odot$  stellar mass cut, this gives 60,957 galaxies with  $0.25 < z < 1$ .

### MORPHOLOGICAL MERGER DETECTION

We measure the following  $r$ -band morphological features (see Goulding et al. 2018) for our galaxies: Sersic index ( $n_{Sersic}$ ), concentration ( $C$ ), asymmetry ( $A$ ), residual asymmetry ( $A_{resid}$ ), residual flux fraction ( $RF$ ), smoothness ( $S$ ), residual smoothness ( $S_{resid}$ ), Gini coefficient ( $G$ ), moment of light ( $M_{20}$ ), and Petrosian radius ( $R_{Petro}$ ). Together with star-formation probability ( $P_{SF}$ , from color-color classification), photo- $z$ ,  $r_{AB}$ , and  $M_*$ , these parameters are used in our Random Forest Classifier (RFC).

We then visually inspect the images of a random, uniform sub-sample of 918 galaxies, to each assigning a merger/non-merger label (136 mergers, 782 non-mergers). This constitutes our training/testing sample (Figure 1(a)). We train the RFC using 70% (642 objects) of our visually-classified sample, and hold back 30% (276) for testing. To balance classes in training, we randomly sub-sample from the non-mergers while up-boosting the merger population by constructing artificial objects based on the features of the identified mergers. The RFC finds that the features in order of decreasing importance are  $RF$ ,  $M_{20}$ ,  $S_{resid}$ ,  $n_{Sersic}$ ,  $C$ ,  $A$ ,  $P_{SF}$ ,  $A_{resid}$ ,  $R_{Petro}$ ,  $S$ ,  $G$ ,  $z_{phot}$ ,  $r_{AB}$ , and  $M_*$ .

For each galaxy, the RFC produces an ensemble of binary classifications, and we take the average of these as the merger probability,  $P_{merge}$ . Testing the RFC output shows that  $P_{merge} > 0.7$  identifies most of the visually-classified mergers, although with a significant fraction of non-merger contaminants (Figure 1(b)). We thus visually inspect the 7,550 objects (13% of the sample) with  $P_{merge} > 0.7$ , yielding 1,576 secure mergers.

### MERGER FRACTION EVOLUTION

Dividing the secure merger numbers by the total galaxy sample gives the *raw, directly observed* merger fraction (open points in Figure 1(c)). However, morphological merger features become harder to detect with increasing redshift, necessitating a redshift-dependent incompleteness correction. We estimate this correction by selecting eight low-redshift mergers from among our images, artificially dimming and spatially resampling them to simulate their appearance at higher redshifts, inserting them into blank-sky regions within our images, and then running the resulting images through our RFC+visual-followup procedure employed previously. The redetection rate gives an estimate of the redshift-dependent incompleteness correction, and the resulting incompleteness-corrected values are shown with filled points in Figure 1(c). Although the size of the uncertainties, particularly at higher redshifts, is now dominated by the Poisson noise in our incompleteness correction measurement, we measure a merger fraction evolution,  $f_{merge}(z) =$

$(0.010 \pm 0.002) \times (1+z)^{2.3 \pm 0.4}$  (Figure 1(c), gray curve), consistent with previous studies (see Table 5.4 of Thibert 2018 for a compilation). Integrating these values suggests that a typical massive galaxy has undergone  $\sim 0.3$  major mergers since  $z = 1$ .

## DISCUSSION AND CONCLUSIONS

Deep ground-based imaging is more sensitive to low surface brightness merger signatures than space-based imaging from HST. Our pilot study points to machine learning as a useful approach to morphologically detecting mergers out to at least  $z \sim 1$  in deep HSC-SSP imaging and similarly-deep datasets (e.g., LSST). In the near future, we will perform ML-based merger detection on the deeper HSC-SSP PDR3 images to study merger fractions as function of redshift, environment, and galaxy evolutionary state.

## REFERENCES

- Ackermann, S., Schawinski, K., Zhang, C., Weigel, A. K., & Turp, M. D. 2018, *MNRAS*, 479, 415, doi: [10.1093/mnras/sty1398](https://doi.org/10.1093/mnras/sty1398)
- Aihara, H., Arimoto, N., Armstrong, R., et al. 2018a, *PASJ*, 70, S4, doi: [10.1093/pasj/psx066](https://doi.org/10.1093/pasj/psx066)
- Aihara, H., Armstrong, R., Bickerton, S., et al. 2018b, *PASJ*, 70, S8, doi: [10.1093/pasj/psx081](https://doi.org/10.1093/pasj/psx081)
- Aihara, H., AlSayyad, Y., Ando, M., et al. 2019, *PASJ*, 71, 114, doi: [10.1093/pasj/psz103](https://doi.org/10.1093/pasj/psz103)
- Bridge, C. R., Carlberg, R. G., & Sullivan, M. 2010, *ApJ*, 709, 1067, doi: [10.1088/0004-637X/709/2/1067](https://doi.org/10.1088/0004-637X/709/2/1067)
- Bundy, K., Fukugita, M., Ellis, R. S., et al. 2009, *ApJ*, 697, 1369, doi: [10.1088/0004-637X/697/2/1369](https://doi.org/10.1088/0004-637X/697/2/1369)
- Conselice, C. J. 2014, *ARAA*, 52, 291, doi: [10.1146/annurev-astro-081913-040037](https://doi.org/10.1146/annurev-astro-081913-040037)
- Conselice, C. J., Rajgor, S., & Myers, R. 2008, *MNRAS*, 386, 909, doi: [10.1111/j.1365-2966.2008.13069.x](https://doi.org/10.1111/j.1365-2966.2008.13069.x)
- Freeman, P. E., Izbicki, R., Lee, A. B., et al. 2013, *MNRAS*, 434, 282, doi: [10.1093/mnras/stt1016](https://doi.org/10.1093/mnras/stt1016)
- Goulding, A. D., Greene, J. E., Bezanson, R., et al. 2018, *PASJ*, 70, doi: [10.1093/pasj/psx135](https://doi.org/10.1093/pasj/psx135)
- Le Fevre, O., Abraham, R., Lilly, S. J., et al. 2000, *MNRAS*, 311, 565–575, doi: [10.1046/j.1365-8711.2000.03083.x](https://doi.org/10.1046/j.1365-8711.2000.03083.x)
- Lotz, J. M., Davis, M., Faber, S. M., et al. 2008, *ApJ*, 672, 177, doi: [10.1086/523659](https://doi.org/10.1086/523659)
- Moutard, T., Sawicki, M., Arnouts, S., et al. 2020, *MNRAS*, 494, 1894, doi: [10.1093/mnras/staa706](https://doi.org/10.1093/mnras/staa706)
- Mundy, C. J., Conselice, C. J., Duncan, K. J., et al. 2017, *MNRAS*, 470, 3507, doi: [10.1093/mnras/stx1238](https://doi.org/10.1093/mnras/stx1238)
- Patton, D. R., Pritchet, C. J., Carlberg, R. G., et al. 2002, *ApJ*, 565, 208, doi: [10.1086/324543](https://doi.org/10.1086/324543)
- Sawicki, M., Arcila-Osejo, L., Golob, A., et al. 2020, *MNRAS*, 494, 1366, doi: [10.1093/mnras/staa779](https://doi.org/10.1093/mnras/staa779)
- Sawicki, M., Arnouts, S., Huang, J., et al. 2019, *MNRAS*, 489, 5202, doi: [10.1093/mnras/stz2522](https://doi.org/10.1093/mnras/stz2522)
- Thibert, N. C. M. 2018, MSc Thesis, Saint Mary's University. <http://library2.smu.ca/handle/01/27980>
- Xu, C. K., Zhao, Y., Scoville, N., et al. 2012, *ApJ*, 747, 85, doi: [10.1088/0004-637X/747/2/85](https://doi.org/10.1088/0004-637X/747/2/85)